Analysis Of VHF Propagation Mechanisms That Cause Interference From The Middle East Within The Southern Coastal Regions Of Cyprus

Antonis Constantinides, Panayiotis Michael

Abstract: Interference is a very important factor in the planning of digital and analog VHF terrestrial radio services. The most common cause of interference in band II & III occurs under line of sight conditions and thus many times can be skipped. Nevertheless, a more complicated case of interference occurs when an unwanted signal travels beyond the horizon due to atmospheric refraction based on specific weather conditions. A case of such abnormal propagation mechanism has been examined in the Mediterranean Sea during the months June, July and August 2015 due to the radio interference which plaguing the southern coast of Cyprus for years. The model based on which calculations were made is the Weather Research Forecasting (WRF-ARW version 3.4). Furthermore, this study utilizes real world measurements in Band II based on current overseas radio transmissions monitored beyond the horizon in clear spectrum during the hot dry months of the summer. The focus was specifically on the field strength variations versus the type of duct favoring the radio waves in Band II, allowing them to travel between the Middle East to beyond the horizon in Cyprus, since line of sight conditions do not exist between the two regions.

Keywords: Abnormal Interference, Propagation Mechanism, Tropospheric Ducting, Refraction.

1. INDRODUCTION

THIS PAPER presents the types of tropospheric ducting that favors the overseas transmissions from the Middle East, allowing them to cause a strong destructive interference in the local radio services along the southern coast of Cyprus during the hot dry months of the summer. The research has been executed as the co-channel and adjacent-channel radio interference degrades the reception quality in major service areas within the cities of Limassol, Paphos, Larnaca and their suburbs, as illustrated on the map presented in Figure 1.

Figure 1: *The Area Affected by Interference from the Middle East*

For example, the interference adversely affects the "in car listening" quality across the main highway that connects the aforementioned cities. Under severe interference conditions, at random locations within the affected area, an automobile receiver demodulates unwanted signals, rather than the desired program to which it has been tuned. Empirical evidence indicates that this phenomenon is more pronounced in motion due to multipath-induced fading. [1] According to the study, the monthly average field strength intensity of the unwanted overseas transmissions fluctuates. However, the graphs demonstrated in this report, indicate that sometimes these effects, exceeds the free space level of the local radio transmissions even in the order of 10dB with duration of few hours when a surface duct causing trapping conditions. Furthermore, the field strength intensity of these unwanted transmissions depends on the weather conditions, and thus varies with the season and the time of reception. For instance, the phenomenon appears weak during the spring and peaks during the hot, dry summer months. During the autumn, the effect weakens again and vanishes completely in the winter. In contrast with other extant propagation mechanism case studies conducted in other regions of the world such as Korea, Nigeria, Japan[2][3][4][8], the model based on which calculations were made in this study is the Weather Research Forecasting (WRF-ARW version 3.4). Furthermore, real world measurements in Band II (87.5 to 108.0 MHz) have been carried out based on existing overseas radio transmissions monitored beyond the horizon in clear spectrum which are given below. The aim was to investigate their characteristics in terms of propagation mechanisms provided by the following ITU Recommendations (ITU-RP.452, 453, and 834) [5][6][7]. These recommendations provide the testing procedures and mathematical expressions incorporating the meteorological parameters that affect the radio refractivity of the Troposphere that permits the overseas radio waves to travel beyond the horizon and cause interference (more details on this phenomenon are provided below).

2. LOCATION AND INSTRUMENTATION SETUP

It was not practically possible to conduct field strength measurements at every single reception point within the southern coast of Cyprus. Consequently, it was important to identify a reference point that can serve as a permanent and reliable source of measurements of field strength intensity of the unwanted overseas transmissions on a daily basis. This was achieved in the northern part of Limassol (34°42'37.14"N, 33° 1'15.26"E). The location is at 393 ft above sea level (asl) and has an absolute line of sight with the coast of Limassol. For reception purposes, a broadband response, -1.5dB gain circular polarized dipole antenna has been installed outdoors, on a mast, one meter above the ground in order to represent the height of a typical commercial receiver's antenna. The testing equipment arrangement is illustrated in Figure 2.

3. MONITORING THE UNWANTED OVERSEAS TRANSMISSIONS

During the study many unwanted overseas transmissions have been monitored in Band II, to overlap with the local radio services, thus, their behavior could not be studied.

Frequency	Location	Path Length	Height	ERP
102.5 MHz	Lebanon	271 km	2995 m	50 kW
95.5 MHz	Israel	376 km	860 m	40 kW
94.8 MHz	Cyprus	29 km	1549 m	30 kW

Table 1: *The Technical Specifications of the Transmitting Signals under study*

Nonetheless, two overseas signals could be detected in a very clear spectrum in Limassol, namely the Lebanon "Radio Libran Libre" 102.5 FM, broadcast from Beirut Lebanon, and the 95.5 MHz, broadcast from Jerusalem, Israel. The technical specifications of the aforementioned overseas signals, versus the national radio Cyprus Broadcasting Corporation "CYBC" are illustrated in table1.

4. THE PATH LENGTH CALCULATIONS OF THE DETECTED SIGNALS

The path length from the aforementioned regions to the coast of Limassol has been determined, by the use of Google Earth professional software tools. The path length between Israel and Limassol, as well as Lebanon and Limassol, has been calculated based on the coordinates given in Figures 3&4. The transmitting point's altitude of the 95.5 MHz signal from Jerusalem is 860 m, and the path length to Limassol is 376 km. Similarly, the path length of the Lebanese 102.5 MHz signal from Beirut measured at 271 km, whereby the transmitting point is located at 2295 m asl.

5. MEASUREMENTS OF 102.5 MHz, 95.5 MHz, AND 94.8 MHz, PERFORMED AT 1:00 PM BETWEEN JUNE 17th AND SEPTEMBER 2nd, 2015

The field strength variations in the 102.5 MHz signal from Beruit (Lebanon) are demonstrated in Figure 5. The measurements have been conducted from June 17th until September 2nd, 2015, at 1:00 PM. During this period, the average field strength intensity of 102.5 MHz was measured at 30 dBuV, and ranged from 10 dBuV to 48 dBuV, with the fluctuations essentially comprising of noise.

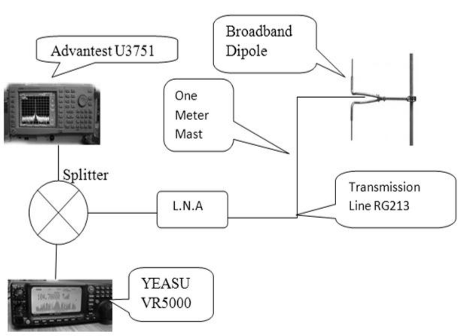

Figure 2: *Testing Equipment Arrangement*

The field strength variation of the aforementioned signal was in the order of 38 dBuV. Similarly, the field strength intensity of the 95.5 MHz signal arriving from Israel was measured between June 17th and September 2nd, 2015, at 1:00 PM, with the data illustrated in Figure 6. The measurements pertaining to the local national radio CYBC signal were performed within the same period as well. The field strength variations of the three signals under study are merged on the graph depicted in Figure 7. The green color represents the field strength intensity of the local 94.8 MHz radio signal, whereas the red and blue lines correspond to the overseas signals at 102.5 MHz and 95.5 MHz, respectively. According to Figure 7, the field strength of the 95.5 MHz prevails over the local radio 94.8 MHz on the specific dates depicted on the graph. Thus, the Carrier-to- interference ratio will determine the interference's density. The worse case occurs when the level of these unwanted signals exceeds that of the local services [8]. Therefore, the worst case scenario of co-channel interference has been established, and is evident from Figure 7, which reveals that the peaks of the overseas 95.5 MHz signal can exceed by approximately 10dBuV the field strength of the CYBC national radio.

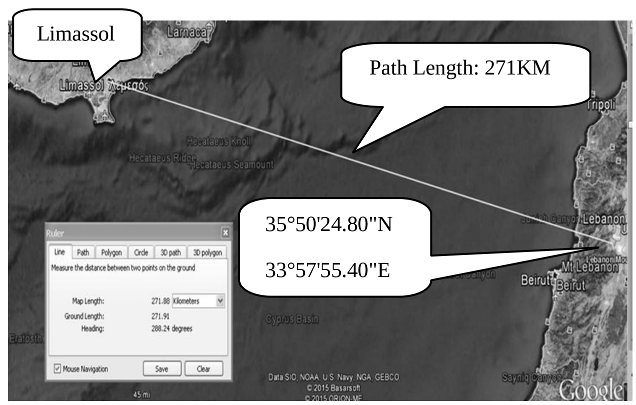

Figure 3: *Path Length between Limassol and Israel,376 km, Height 860 m*

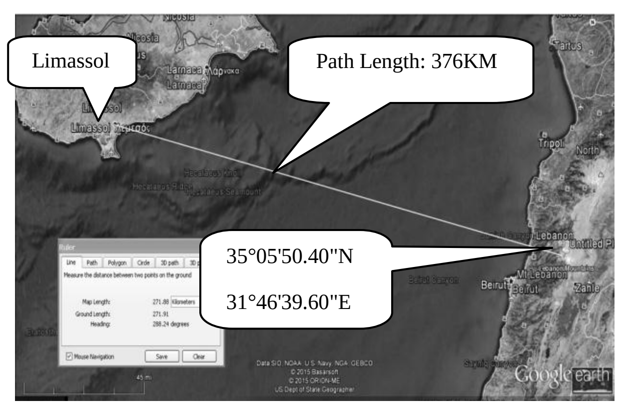

Figure 4: *Path Length between Limassol and Lebanon, 271 km, Height 2995 m*

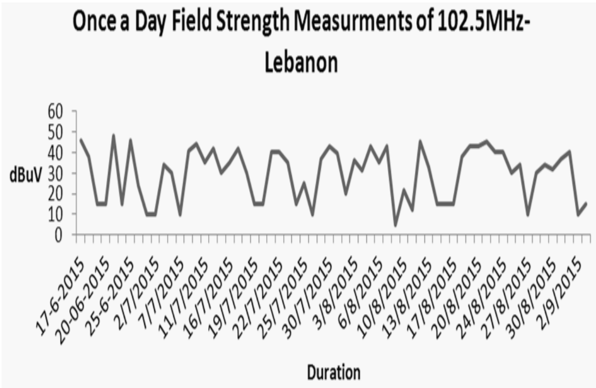

Figure 5: *The Field Strength Intensity of 102,5 MHz*

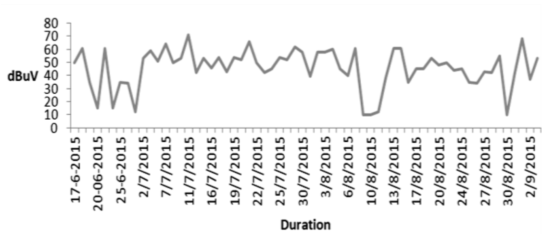

Figure 6: *The Field Strength Intensity of 95.5 MHz*

Figure 8 illustrates the variations in this phenomenon and elucidates the cause of a severe interference, which would occur in the evening on the given dates, provided that the local radio services would share the same spectrum as that adopted by the overseas signals.

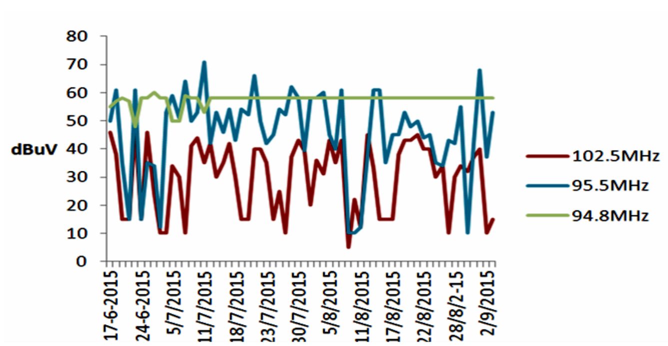

Figure 7: *The Field Strength Intensity of the Three Signals under Study*

6. SHORT-TERM MEASUREMENTS OF THE 95.5 MHz AND 94.8 MHz SIGNALS CONDUCTED BETWEEN JUNE 17th TO SEPTEMBER 2nd, 2015, FROM 11:00 AM TO 7:00 PM

Figure 9 illustrates the field strength variations of 95.5 MHz signal between 11:00 AM to7:00 PM, based on the measurements conducted on August 24th and 25th, 2015.

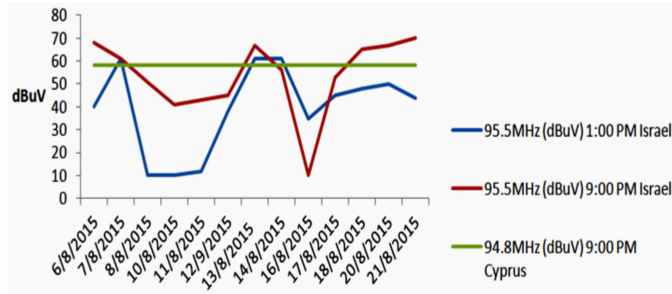

Figure 8: *The Field Strength Variations in the 95.5 MHz and 94.8 MHz Signal, as Measured at 1:00 and 9:00 PM*

These measurements revealed that the field strength intensity of the overseas signal was sporadic, i.e. comprised of various values. An important observation is that its intensity measured on August 24th at 4:00 PM exceeded the free space value of the local national radio services CYBC, whereas the values were below the reference value at all other times.

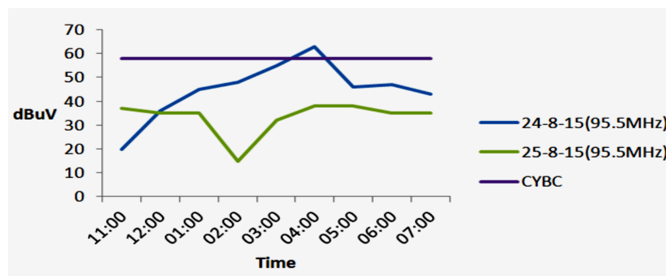

Figure 9: *The Field Strength Variations of the 95.5 MHz and 94.8 MHz Signals, as measured between 11:00 and 7:00 PM*

The average field intensity measurements of the monitored 95.5 MHz signal from Israel during the summer months (June, July and August) are illustrated in Figure 10 below.

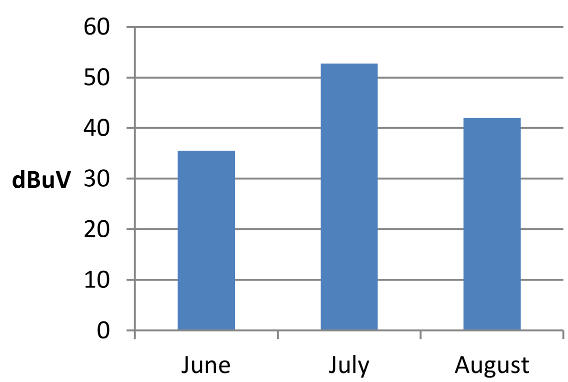

Figure 10: *Average Field Intensity of 95.5MHz during summer 2015*

However, it is noteworthy that the average field intensity of the 102.5 MHz signal arriving from Lebanon (illustrated in Figure 11) is different from the 95.5 MHz signal. The field has an average intensity of 13 dBuV in June, after which it increases to 31 dBuV in July, before declining to 30 dBuV in August

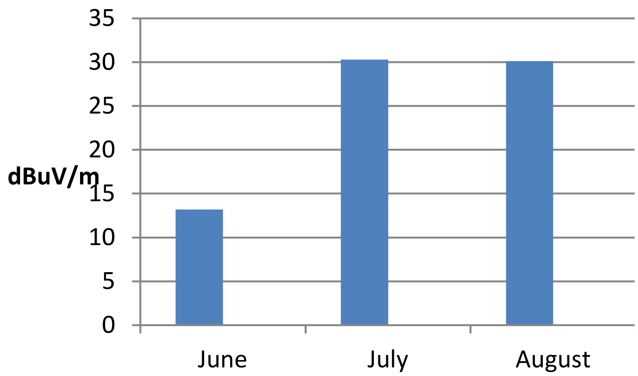

Figure 11: *Average Field Intensity of 102.5 MHz during summer 2015*

7. THE TYPE OF DUCTS ALONG THE LIMASSOL COAST

This chapter presents the results obtained by the Meteorological Department of Cyprus during the periods of very strong, medium and low field strength intensity of the overseas monitored signals discussed before. The coordinates under investigation for the radio signals transmitted at frequencies of 95.5 and 102.5 MHz are illustrated in fig.10

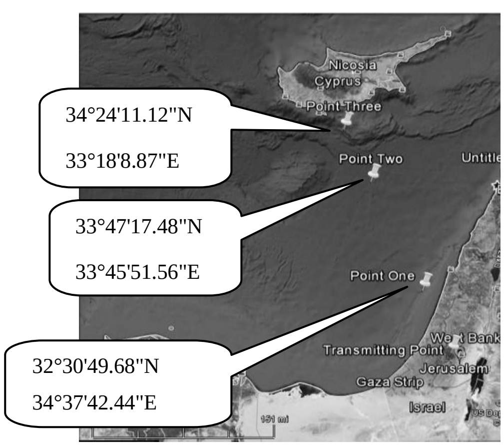

Figure 10: *The coordinates under investigation for the radio signals transmitted at frequencies of 95.5 and 102.5 MHz*

The model based on which calculations were made is the WRF-ARW, version 3.4. The calculations were made to 18 km distance grid initially / boundary data from the Global Forecasting System (GFS) with a resolution of 0.5 degrees and time step boundary conditions three hours . The step integration was not fixed but adaptive / dynamic, based on the criterion CFL. The number of vertical planes (eta levels / terrain following) was 60. The configurations used are given below:

1. Micro-physics: WRF Single-moment 3-class scheme
2. Radiation longwave: Rapid Radiative Transfer Model
3. Radiation shortwave: Dudhia Scheme
4. Surface layer: MM5 / Monin-Obukhov Scheme
5. Boundary layer: Yonsei University Non-local-K scheme
6. Cumulus / convection: Kain-Fritsch scheme.

For the aforementioned, the main goal is to provide evidence-based explanation for the radio interference observed along the southern coast of Cyprus. As a result, the refractivity N can be obtained based on the Recommendation ITU-R P.453-8 by applying Equation 1 below:

$$N = N_{dry} + N_{wet} = \frac{77.6}{T}\left[P + 4810\frac{e}{T}\right] \text{ N-Units} \qquad \text{Eq. (1)}$$

Where P denotes atmospheric pressure (hpa), e represents water vapor pressure (hpa), T is absolute temperature (K), and RH is relative humidity expressed in %.

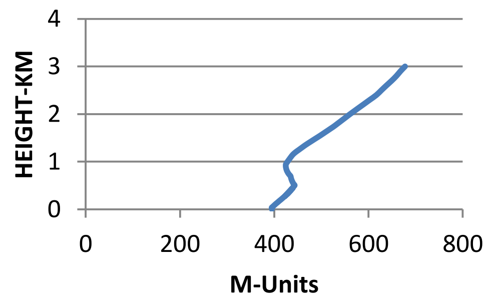

Figure 12: *Temperature inversion on 06-Aug-15 at Point 3*

Based on equation 1, trapping occurs when the N gradient exceeds -157 N/km. However, the same meteorological conditions cause trapping and super refraction interference. In this regard, the difference between trapping and super refraction pertains to the radius of the propagated wave, which becomes smaller than the Earths' radius as it decreases beyond the critical gradient. In such case, the electromagnetic waves are trapped within a thin layer of the troposphere, denoted as duct. When the wave is trapped in this tropospheric channel, its energy can propagate over great ranges. Furthermore, according to the Rec. ITU-R P.453-8, ducts can be described in terms of modified refractivity which is expressed by the equation below:

M(h) defined by Equation 2 :

$$M(h) = N(h) + 157h \text{ (M-units)} \qquad \text{Eq. (2)}$$

where h (km) is the height.

Applying equation 2 denotes an elevated duct in fig.12 a surface based duct in fig.13 and a surface duct in figure 14. This phenomenon can be explained as the air aloft is very warm compared to the temperature of the sea. Thus, the surface-based ducts occur. For example, they can arise due to the hot air masses that pass over the cool water surface of the Mediterranean Sea. On the other hand, elevated ducts occur when the meteorological conditions are favorable for such phenomena to occur aloft above the Earth's surface.

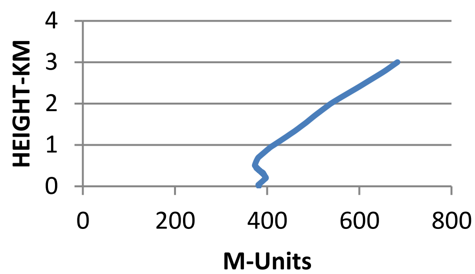

Figure 13: *Surface Based Duct measurements made on 11-Aug-15 at Point 3.*

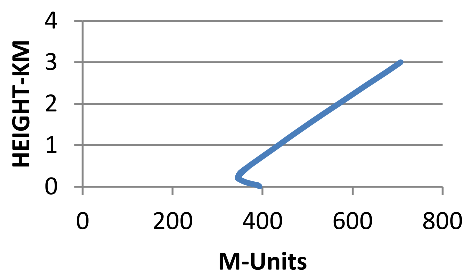

Figure 14: *Surface Duct measurements made on 08-Jul-15 at Point 3.*

I. CHAPTER CONCLUSION

From this study, it has emerged that with the aid of the WRF-ARW, version 3.4 may predict the level of interference of at least 10 hours foregoing without needing other meteorological complicated procedures. This is verified by the intersection of the results of signal intensity with the meteo conditions that create the ducts. Within this context, it has also emerged that the type and amount of Duck plays a very important role in signal intensity. The findings presented in this paper revealed that the radio interference experienced along the southern coast of Cyprus is caused by three major types of ducts. Presence of these ducts has been verified close to the coast of Limassol, whereby they were classified as surface, surface based and elevated ducts. According to the interference assessment performed on specific dates, it can be posited that strong temperature inversion is directly proportional to strong radio interference in close proximity to the coast of Limassol. Moreover, the study results have shown the electromagnetic waves in Band II can travel through the ducts with stronger field strength intensity of the free space value when the elevation of the duct approaches the Earth's surface. Particularly, according to the findings presented in this paper, the field strength intensity exceeds the free space value by approximately 10 dB. On the other hand, when there is no temperature inversion, a very low interference effect or its complete absence was noted.

REFERENCES

[1] D. K. Chy, 'Evaluation of SNR for AWGN, Rayleigh and Rician Fading Channels Under DPSK Modulation Scheme with Constant BER', International Journal of Wireless Communications and Mobile Computing, vol. 3, no. 1, p. 7, 2015.

[2] H. Son, J. Kim and C. Kim, Journal of the Korean institute of electromagnetic engineering and science, vol. 12, no. 1, pp. 94-100, 2012.

[3] M. Nishi, H. Shinbara, K. Shin and T. Yoshida, 'Observation results of non-line-of sight 77.1 MHz FM radio waves on three different paths for three years', Journal of Atmospheric Electricity, vol. 31, no. 1, pp. 11-22, 2011.

[4] 'Terrestrial microwave radio relay system development at frequencies above 10 Ghz', Radio Electron. Eng. UK, vol. 42, no. 4, p. 195, 1972.

[5] RECOMMENDATION ITU-R P.452-11(2003), Prediction procedure for the evaluation of microwave interference between stations on the surface of the Earth at frequencies above about 0.7 GHz

[6] RECOMMENDATION ITU-R P.453-8(2001), The radio refractive index: its formula and refractivity data.

[7] RECOMMENDATION ITU-R P.834-4(2003), Effects of tropospheric refraction on radiowave propagation.

[8] P. Petrov, 'Prediction of interference by modeling a radio interference meter', Measurement Techniques, vol. 37, no. 6, pp. 676-683, 1994.

[9] C. Sim and E. Warrington, 'Signal strength measurements at frequencies of around 300 MHz over two sea paths in the British Channel Islands', Radio Sci., vol. 41, no. 3, p. n/a-n/a, 2006.

[10] `D. Siddle and E. Warrington, 'Diurnal changes in UHF propagation over the English Channel', Electron. Lett, vol. 41, no. 21, p. 1152, 2005.